

Supplement of Atmos. Chem. Phys., 20, 12459–12482, 2020
<https://doi.org/10.5194/acp-20-12459-2020-supplement>
© Author(s) 2020. This work is distributed under
the Creative Commons Attribution 4.0 License.



Supplement of

Ice-nucleating particle concentrations of the past: insights from a 600-year-old Greenland ice core

Jann Schrod et al.

Correspondence to: Jann Schrod (schrod@iau.uni-frankfurt.de)

The copyright of individual parts of the supplement might differ from the CC BY 4.0 License.

Extended description of “Conversion to atmospheric concentrations”

To convert the cumulative INP concentration per volume of meltwater to an atmospheric concentration, we follow the theoretical considerations presented in Fischer et al. (2007). As for any aerosol particle, an INP can be transferred from the air to the surface of the ice sheet either by dry deposition (predominantly gravitational settling and turbulent transport) and wet deposition (cloud particle activation or riming and subsequent removal by precipitation, or below-cloud scavenging). Fischer et al. (2007) states that in a simplified model the total deposition flux J_{ice} (i.e. the sum of the flux of dry and wet deposition, J_{dry} and J_{wet} , respectively) to the ice surface is defined by the product of the snow accumulation rate A and the average concentration of the investigated species (i.e. here for INPs: $N_{INP_{ice}}$) in the ice core sample. Over long periods of time the deposition flux can be written as:

$$J_{ice} = A \cdot N_{INP_{ice}} = J_{dry} + J_{wet} = v_{dry} \cdot N_{INP_{atm}} + A \cdot \varepsilon \cdot N_{INP_{atm}}, \quad (1)$$

where $N_{INP_{atm}}$ is the atmospheric INP concentration (or any other investigated species of interest), v_{dry} is the dry deposition velocity and ε is the effective scavenging efficiency including in-cloud and below-cloud scavenging. Experimentally, ε is often defined as particle concentration in cloud water or in precipitation (snow/ice/rain) divided by the airborne particle concentration. Rearranging Eq. 1 leads to:

$$N_{INP_{atm}} = \frac{N_{INP_{ice}}}{\frac{v_{dry}}{A} + \varepsilon}. \quad (2)$$

Thus, it is possible to calculate the (Arctic) atmospheric INP concentration, when realistic values for the variables A , v_{dry} and ε are estimated. However, Eq. 2 implies that if deposition fluxes change over the time span of the ice core (in particular the wet deposition, which is directly related to changes in the precipitation rate), the concentration of the investigated species in the ice will change as well. This means that not all potential changes seen in the ice core INP concentration, are necessarily caused by actual changes in the atmospheric concentration. Henceforth, we will, however, treat these variables as constants due to the lack of a better knowledge and because climate conditions changed only little over the last centuries. In particular, the average snow accumulation of the B17 ice core has been determined by Weißbach et al. (2016) and shows little variation over time ($A = 11.4 \pm 0.1$ cm water equivalent a^{-1} , $N = 630$). Unfortunately, the other deposition parameters are not as well-known.

In general, v_{dry} heavily depends on the particle diameter, shape, density and physical properties of the particle. The typical range is between 10^{-2} $cm\ s^{-1}$ and 10 $cm\ s^{-1}$ (Seinfeld and Pandis, 2006). Smaller particles ($d_p < 0.1$ μm) and larger particles ($d_p > 1$ μm) usually have higher dry deposition velocities than medium sized particles, where Brownian diffusion and gravitational settling are low (Davidson et al., 1996). Moreover, the nature of the surface itself (e.g. surface type and smoothness) and the level of atmospheric turbulence at the nearest layer to the ground have a major influence on v_{dry} (Seinfeld and Pandis, 2006). Moreover, over the ice sheet, the dry deposition is strongly influenced by snow ventilation effects induced by surface roughness (Cunningham and Waddington, 1993). Khan and Perlinger (2017) evaluated five different dry deposition parametrizations with respect to their ability to accurately explain field observations from five land use categories (snow/ice: 8 studies). The parametrization by Zhang and He (2014) performed best overall, and best for snow/ice covered surfaces in particular. Therefore, we used the parametrization by Zhang and He (2014)(Eq. 4) to estimate the dry deposition velocity for $PM_{2.5}$ aerosol particles. The parametrization is predominantly dependent on the so-called friction velocity u_* and the particle diameter d_p . Khan and Perlinger (2017) use a value $u_* = 0.12$ $m\ s^{-1}$ for snow/ice surfaces in their observation based accuracy test evaluation. We decided to set d_p in the parametrization to 0.5 μm , since particles of this size and larger are typically considered to be “good” INPs (DeMott et al., 2010, 2015). Osman et al. (2017) analyzed *modern day* samples from two ice cores from west-central Greenland with a time-of-flight single-particle mass spectrometer to determine the size and composition of insoluble particles. The median particle diameter of insoluble particles within the detectable aerodynamic size range of $0.2 - 3$ μm was about 520 nm (mean 595 $nm \pm 360$ nm , $N = 8021$), which agrees well with our assumption. Filling in the other variables given in Zhang and He (2014) and Khan and Perlinger (2017), we find a dry deposition velocity of $v_{dry} = 0.05$ $cm\ s^{-1}$. This value agrees well with the dry deposition velocity of 0.03 $cm\ s^{-1}$, which is used for all aerosols over snow and ice surfaces in the GEOS-chem model (GEOS-Chem, 2011).

The scavenging efficiency ε (also known as scavenging ratio or washout ratio) is even less well known than the dry deposition velocity. The scavenging ratio is a very complex parameter that is controlled by the particle’s size, its physical shape and

chemical composition, as well as by cloud properties such as droplet size, cloud temperature and cloud type, and by the vertical extent of rain and cloud (Duce et al., 1991; Shao, 2008). Hence, accurate predictions of ε are very difficult (Shao, 2008). Duce et al. (1991) warns that experimentally determined concentrations at the ground do not necessarily have to reflect the conditions near the cloud, where the particles are mainly scavenged. Furthermore, ε can vary greatly for different particle species and should therefore be assessed carefully (Duce et al., 1991). Attention should also be paid to the fact that ε is reported in the literature either in a mass- or volume-based dimension ($(g_{\text{species}}/g_{\text{precip}})/(g_{\text{species}}/g_{\text{air}})$ vs. $(g_{\text{species}}/\text{cm}^{-3}_{\text{precip}})/(g_{\text{species}}/\text{cm}^{-3}_{\text{air}})$). These two definitions differ by the factor $\rho_{\text{precip}}/\rho_{\text{air}}$ (ε_{vol} is about 1000 times higher than $\varepsilon_{\text{mass}}$). Usually, ε is calculated by measuring the airborne concentration of a species and its concentration in a precipitation sample simultaneously at the ground. The volume-based scavenging ratio is typically in the range of 10^5 to 10^6 (Slinn et al., 1978). Mass-based scavenging ratios for mineral aerosols are typically somewhere between 100 and 2000 (Duce et al., 1991). Davidson et al. (1996) reported Arctic $\varepsilon_{\text{mass}}$ for Ca to be 840 for Summit, Greenland. For the purpose of this manuscript we use a value for ε that is derived from long time observations by Cheng and Zhang (2017). They measured the scavenging ratio for various species at 13 Canadian stations for several years. They give a long-time average value for several species, each composed of individual means from months that experienced at least 15 days with more than 0.2 mm of precipitation. The combined measured concentrations of Ca^{2+} , Mg^{2+} , and Na^+ can be taken as a proxy for coarse particulate aerosols (e.g. mineral dust). The long-time average of all 13 stations of these three species yields $\varepsilon_{\text{mass}} \approx 1.12 \cdot 10^3$, which we will use for the scavenging ratio in this manuscript. Note, that the densities of air and water, which are part of the definition of ε , depend on temperature and altitude. Here, we assumed the densities of air ρ_{air} and water ρ_{water} to be 1.01 kg m^{-3} (-25°C , 2820 m) and 1000 kg m^{-3} , respectively. This yields a ε_{vol} of $1.11 \cdot 10^6$. Moreover, technically ε_{vol} compares the mass and not the number of a certain species within a volume of water and air. INP concentrations, however, give the number of ice-active particles per volume. Considering the large uncertainties accompanied with the scavenging ratio, we disregard this inconsistency.

Following these assumptions, we obtain a factor of about $8 \cdot 10^{-7}$ for converting from N_{INPice} to N_{INPatm} (Fig. 4, blue cross). Figure 4a displays the range of the possible conversion factors as a result of other combinations of v_{dry} and ε . Figure 4b shows the sensitivity of the chosen conversion factor associated with the uncertainties in dry and wet deposition efficiencies. Judging from the typical range of literature values of v_{dry} and ε , the uncertainty of the conversion factor is likely within $\pm 50\%$ of our best estimate. Likewise, our conversion factor is only about twice as high as the conversion factor proposed in Petters and Wright (2015), who compiled INP data from precipitation measurements and translated these to atmospheric INP concentrations at cloud level. Petters and Wright (2015) based their estimation on the assumption that cloud droplets of typically 1 pL (each containing no more than one INP) dispersed in 1 m^3 of air weigh about 0.4 g (cloud water content (CWC) ranges between 0.2 and 0.8 g m^{-3}). Depending on the exact CWC, the uncertainty of the Petters and Wright (2015) estimation is also a factor of 2.

Similar to what we propose here, Schüpbach et al. (2018) successfully implemented the assumptions described above into a trajectory based source apportionment study to translate ice core concentrations of Na^+ , Ca^{2+} , NH_4^+ , NO_3^- and SO_4^{2-} to atmospheric source concentrations for a 130k year record of Greenland ice core aerosol data.

References

- Cheng, I., and Zhang, L.: Long-term air concentrations, wet deposition, and scavenging ratios of inorganic ions, HNO₃, and SO₂ and assessment of aerosol and precipitation acidity at Canadian rural locations, *Atmos. Chem. Phys.*, 17, 4711–4730, <https://doi.org/10.5194/acp-17-4711-2017>, 2017.
- 5 Cunningham, J., and Waddington, E. D.: Air flow and dry deposition of non-sea salt sulfate in polar firm: paleoclimatic implications, *Atmospheric Environment*, 27, 17–18, 2943–2956, [https://doi.org/10.1016/0960-1686\(93\)90327-U](https://doi.org/10.1016/0960-1686(93)90327-U), 1993.
- Davidson, C. I., Bergin, M. H., and Kuhns, H. D.: The Deposition of Particles and Gases to Ice Sheets, in: *Chemical Exchange Between the Atmosphere and Polar Snow*, edited by: Wolff, E. W., and Bales R. C., Springer, Berlin, Heidelberg, Germany, 275–306, https://doi.org/10.1007/978-3-642-61171-1_12, 1996.
- 10 DeMott, P. J., Prenni, A. J., Liu, X., Kreidenweis, S. M., Petters, M. D., Twohy, C. H., Richardson, M. S., Eidhammer T., and Rogers, D. C.: Predicting global atmospheric ice nuclei distributions and their impacts on climate, *PNAS*, 107, 25, 11217–11222, <https://doi.org/10.1073/pnas.0910818107>, 2010.
- DeMott, P. J., Prenni, A. J., McMeeking, G. R., Sullivan, R. C., Petters, M. D., Tobo, Y., Niemand, M., Möhler, O., Snider, J. R., Wang, Z., and Kreidenweis, S. M.: Integrating laboratory and field data to quantify the immersion freezing ice nucleation activity of mineral dust particles, *Atmos. Chem. Phys.*, 15, 393–409, <https://doi.org/10.5194/acp-15-393-2015>, 2015.
- 15 Duce, R. A., Liss, P. S., Merrill, J. T., Atlas, E. L., Buat-Menard, P., Hicks, B. B., Miller, J. M., Prospero, J. M., Arimoto, R., Church, T. M., Ellis, W., Galloway, J. N., Hansen, L., Jickells, T. D., Knap, A. H., Reinhardt, K. H., Schneider, B., Soudine, A., Tokos, J. J., Tsunogai, S., Wollast, R., and Zhou, M.: The atmospheric input of trace species to the world ocean, *Global Biogeochem. Cycles*, 5, 3, 193–259, <https://doi.org/10.1029/91GB01778>, 1991.
- 20 Fischer, H., Siggaard-Andersen, M.-L., Ruth, U., Röthlisberger, R., and Wolff, E.: Glacial/interglacial changes in mineral dust and sea-salt records in polar ice cores: Sources, transport, and deposition, *Rev. Geophys.*, 45, RG1002, <https://doi.org/10.1029/2005RG000192>, 2007.
- GEOS-Chem dry deposition scheme: http://wiki.seas.harvard.edu/geos-chem/index.php/Dry_deposition#Aerosol_dry_deposition_velocities_over_snow_and_ice_surfaces, last access: 27 January 2020, 2011.
- Khan, T. R., and Perlinger, J. A.: Evaluation of five dry particle deposition parameterizations for incorporation into atmospheric transport models, *Geosci. Model Dev.*, 10, 3861–3888, <https://doi.org/10.5194/gmd-10-3861-2017>, 2017.
- 25 Osman, M., Zawadowicz, M. A., Das, S. B., and Cziczo, D. J.: Real-time analysis of insoluble particles in glacial ice using single-particle mass spectrometry, *Atmos. Meas. Tech.*, 10, 4459–4477, <https://doi.org/10.5194/amt-10-4459-2017>, 2017.
- Petters, M. D., and Wright, T. P.: Revisiting ice nucleation from precipitation samples, *Geophys. Res. Lett.*, 42, 8758–8766, <https://doi.org/10.1002/2015GL065733>, 2015.
- 30 Schüpbach, S., Fischer, H., Bigler, M., Erhardt, T., Gfeller, G., Leuenberger, D., Mini, O., Mulvaney, R., Abram, N. J., Fleet, L., Frey, M. M., Thomas, E., Svensson, A., Dahl-Jensen, D., Kettner, E., Kjaer, H., Seierstad, I., Steffensen, J. P., Rasmussen, S. O., Vallelonga, P., Winstrup, M., Wegner, A., Twarloh, B., Wolff, K., Schmidt, K., Goto-Azuma, K., Kuramoto, T., Hirabayashi, M., Uetake, J., Zheng, J., Bourgeois, J., Fisher, D., Zhiheng, D., Xiao, C., Legrand, M., Spolaor, A., Gabrieli, J., Barbante, C., Kang, J.-H., Hur, S. D., Hong, S. B., Hwang, H. J., Hong, S., Hansson, M., Iizuka, Y., Oyabu, I., Muscheler, R., Adolphi, F., Maselli, O., McConnell, J., and Wolff, E.
- 35 W.: Greenland records of aerosol source and atmospheric lifetime changes from the Eemian to the Holocene, *Nature Communications*, 9, 1476, <https://doi.org/10.1038/s41467-018-03924-3>, 2018.
- Seinfeld, J. H. and Pandis, S. N. (Eds.): *Atmospheric Chemistry and Physics: From Air Pollution to Climate Change*. 2nd Edition, John Wiley & Sons, New York, USA, 2006.
- Shao, Y.: Dust Transport and Deposition, in: *Physics and Modelling of Wind Erosion*. Atmospheric and Oceanographic Sciences Library, vol 40 37, edited by: Shao, Y., Springer, Dordrecht, Germany, 247–301, https://doi.org/10.1007/978-1-4020-8895-7_8, 1996.
- Slinn, W. G. N., Hasse, L., Hicks, B. B., Hogan, A. W., Lal, D., Liss, P.S., Munnich, K.O., Sehmel, G.A., and Vittori, O.: Some aspects of the transfer of atmospheric trace constituents past the air-sea interface, *Atmospheric Environment*, 12, 11, 2055–2087, [https://doi.org/10.1016/0004-6981\(78\)90163-4](https://doi.org/10.1016/0004-6981(78)90163-4), 1978.
- Weißbach, S., Wegner, A., Opel, T., Oerter, H., Vinther, B. M., and Kipfstuhl, S.: Spatial and temporal oxygen isotope variability in northern Greenland – implications for a new climate record over the past millennium, *Clim. Past*, 12, 171–188, <https://doi.org/10.5194/cp-12-171-2016>, 2016.
- Zhang, L., and He, Z.: Technical Note: An empirical algorithm estimating dry deposition velocity of fine, coarse and giant particles, *Atmos. Chem. Phys.*, 14, 3729–3737, <https://doi.org/10.5194/acp-14-3729-2014>, 2014.

Table S1: List of ice nucleation samples from the B17 ice core analyzed in this study.

Sample Identifier	Depth from the top [m]	Estimated Year	Time coverage [a]	Data Group according to Fig. 1
6L	1.21	1989.7	0.8	10 year samples, 1990 - 1960 reference
8L	1.65	1988.5	0.3	1990 - 1960 reference
11L	1.89	1987.8	0.5	1990 - 1960 reference
13L	2.46	1986.2	0.6	1990 - 1960 reference
15L	2.70	1985.5	0.3	1990 - 1960 reference
18L	3.00	1984.8	0.5	1990 - 1960 reference
19L	3.26	1983.5	0.8	1990 - 1960 reference
21L	3.62	1982.8	0.4	1990 - 1960 reference
24L	3.90	1982.0	0.7	1990 - 1960 reference
26L	4.41	1980.4	0.4	1990 - 1960 reference
28L	4.64	1979.6	0.2	10 year samples, 1990 - 1960 reference
29L	4.72	1979.5	0.9	1990 - 1960 reference
30L	5.12	1977.7	2.0	1990 - 1960 reference
31L	5.72	1975.5	1.2	1990 - 1960 reference
34L	6.14	1974.7	0.3	1990 - 1960 reference
36L	6.31	1973.8	0.5	1990 - 1960 reference
38L	6.38	1973.6	0.5	1990 - 1960 reference
39L	6.59	1972.6	0.5	1990 - 1960 reference
41L	6.96	1971.8	0.3	1990 - 1960 reference
44L	7.34	1970.0	0.9	1990 - 1960 reference
45L	7.59	1969.6	0.4	10 year samples, 1990 - 1960 reference
47L	7.79	1968.9	0.3	1990 - 1960 reference
51L	8.15	1967.3	0.5	1990 - 1960 reference
52L	8.30	1967.2	0.5	1990 - 1960 reference
53L	8.50	1966.2	0.9	1990 - 1960 reference
55L	8.86	1964.9	0.4	1990 - 1960 reference
58L	9.12	1963.7	0.5	1990 - 1960 reference
60L	9.44	1962.2	1.0	1990 - 1960 reference
61L	9.69	1961.8	0.4	1990 - 1960 reference
63L	9.90	1961.0	0.3	1990 - 1960 reference
66L	10.16	1960.0	0.5	10 year samples, 1990 - 1960 reference
84L	12.59	1950.1	0.4	10 year samples
107L	14.56	1941.6	0.4	other
113L	14.92	1940.0	0.5	10 year samples
141L	17.42	1928.6	0.4	10 year samples
161L	19.16	1919.7	1.0	10 year samples
182L	21.15	1909.8	1.0	10 year samples, volcanic events
209L	23.15	1899.5	1.0	10 year samples
232L	25.14	1888.9	1.0	10 year samples
254L	26.93	1879.7	0.5	10 year samples
276L	28.75	1869.5	0.4	10 year samples
278L	28.89	1868.7	0.3	dust events
279L	28.95	1868.4	0.2	dust events
281L	29.15	1866.7	1.0	dust events
282L	29.33	1866.2	0.4	dust events

Table S1: ...continued

283L	29.40	1865.8	0.4	dust events
297L	30.47	1859.7	0.5	10 year samples
332L	32.18	1849.4	0.5	10 year samples
356L	33.93	1839.3	0.4	10 year samples
378L	35.59	1829.2	0.4	10 year samples
402L	37.26	1819.0	0.4	10 year samples
423L	38.84	1809.4	0.4	10 year samples
447L	40.47	1799.5	0.4	10 year samples
472L	42.07	1789.7	0.4	10 year samples
475L	42.27	1788.5	0.4	volcanic events
478L	42.47	1787.1	0.5	volcanic events
480L	42.62	1786.3	0.4	volcanic events
482L	42.75	1785.5	0.4	volcanic events
485L	42.94	1784.4	0.4	volcanic events
487L	43.07	1783.6	0.4	volcanic events
488L	43.14	1783.1	0.4	volcanic events
489L	43.20	1782.7	0.4	volcanic events
490L	43.27	1782.3	0.5	volcanic events
491L	43.34	1781.8	0.4	volcanic events
495L	43.60	1780.1	0.5	10 year samples
519L	45.18	1770.0	0.4	10 year samples
23H	46.69	1760.2	0.1	10 year samples
116H	48.21	1750.2	0.1	10 year samples
545L	49.74	1739.9	0.4	10 year samples
566L	51.21	1730.1	0.4	10 year samples
589L	52.68	1720.2	0.4	10 year samples
612L	54.15	1710.2	0.6	10 year samples
621L	54.82	1705.6	0.4	other
629L	55.41	1701.6	0.4	other
632L	55.59	1700.2	0.5	10 year samples
655L	57.04	1690.3	0.4	10 year samples
677L	58.46	1680.2	0.5	10 year samples
698L	59.87	1670.2	0.3	10 year samples
721L	61.31	1659.8	0.4	10 year samples
743L	62.73	1649.6	0.5	10 year samples
763L	64.08	1639.7	0.5	10 year samples
781L	65.46	1629.7	0.5	10 year samples
803L	66.86	1619.6	0.5	10 year samples
826L	68.25	1609.4	0.5	10 year samples
849L	69.59	1599.6	0.4	10 year samples
874L	70.97	1589.5	0.5	10 year samples
897L	72.32	1579.5	0.4	10 year samples
921L	73.70	1569.3	0.5	10 year samples
945L	75.05	1559.2	0.4	10 year samples
968L	76.35	1549.6	0.4	10 year samples
994L	77.72	1539.4	0.4	10 year samples
1019L	79.04	1529.4	0.4	10 year samples

Table S1: ...continued

1041L	80.34	1519.8	0.4	10 year samples
1063L	81.67	1509.7	0.5	10 year samples
1089L	82.98	1499.9	0.5	10 year samples
1108L	84.32	1489.7	0.5	10 year samples
1131L	85.64	1479.7	0.5	10 year samples
1133L	85.77	1478.6	0.5	volcanic events, dust events
1135L	85.90	1477.8	0.5	volcanic events, dust events
1137L	86.03	1476.7	0.5	volcanic events, dust events
1139L	86.15	1475.8	0.4	volcanic events, dust events
1140L	86.21	1475.4	0.4	volcanic events, dust events
1141L	86.27	1475.0	0.4	volcanic events, dust events
1142L	86.32	1474.5	0.4	volcanic events, dust events
1143L	86.38	1474.1	0.4	volcanic events, dust events
1152L	86.91	1470.1	0.4	10 year samples
207H	87.65	1464.8	0.1	seasonal resolution
208H	87.66	1464.6	0.1	seasonal resolution
209H	87.68	1464.5	0.1	seasonal resolution
210H	87.69	1464.4	0.1	seasonal resolution
211H	87.71	1464.3	0.1	seasonal resolution
212H	87.72	1464.2	0.1	seasonal resolution
214H	87.75	1464.0	0.1	seasonal resolution
215H	87.77	1463.9	0.1	seasonal resolution
216H	87.78	1463.7	0.1	seasonal resolution
218H	87.81	1463.5	0.1	seasonal resolution
219H	87.83	1463.4	0.1	seasonal resolution
220H	87.85	1463.2	0.1	seasonal resolution
245H	88.24	1460.2	0.1	10 year samples
1198H	89.57	1450.0	0.1	10 year samples
1199H	89.59	1449.9	0.1	other
1284H	90.84	1440.5	0.1	10 year samples
1326L	92.15	1430.1	0.7	10 year samples
1348L	93.45	1420.1	0.5	10 year samples
1372L	94.80	1409.7	0.4	10 year samples
1392M	95.53	1404.3	0.2	dust events
1393M	95.55	1404.1	0.2	dust events
1394M	95.58	1403.9	0.2	dust events
1395M	95.61	1403.7	0.2	dust events
1396M	95.63	1403.5	0.2	dust events
1397M	95.66	1403.3	0.2	dust events
1413M	96.09	1400.0	0.2	10 year samples
1460M	97.40	1389.9	0.2	10 year samples
1509M	98.71	1379.7	0.2	10 year samples
1558M	100.04	1369.5	0.2	10 year samples

Table S2. Pearson correlation between the INP concentration and selected CFA parameters of indicated subsets of the data (“events” include the groups dust, volcanic and seasonal, cf. Fig. 1). Bold coefficients indicate a significant correlation ($p < 0.05$). The number of samples is given in parenthesis.

T [°C]	10 years			modern day			events		
	dust	conductivity	Ca ²⁺	dust	conductivity	Ca ²⁺	dust	conductivity	Ca ²⁺
-20	-0.20 (18)	0.12 (19)	-0.29 (19)	-0.37 (11)	-0.09 (11)	-0.08 (11)	-0.01 (25)	-0.01 (25)	-0.06 (25)
-21	-0.13 (37)	0.04 (38)	-0.19 (38)	-0.25 (17)	-0.35 (17)	-0.44 (16)	0.35 (34)	0.44 (34)	0.29 (34)
-22	-0.05 (46)	-0.08 (47)	-0.05 (47)	-0.16 (23)	-0.27 (23)	-0.38 (22)	0.29 (39)	0.15 (39)	0.21 (39)
-23	0.02 (53)	-0.08 (54)	-0.06 (54)	-0.17 (23)	-0.27 (23)	-0.40 (22)	0.23 (42)	0.18 (42)	0.16 (42)
-24	0.00 (57)	-0.04 (58)	-0.06 (58)	-0.12 (23)	-0.21 (23)	-0.35 (22)	0.34 (42)	0.22 (42)	0.25 (42)
-25	0.01 (57)	-0.08 (58)	-0.11 (58)	-0.09 (23)	-0.21 (23)	-0.37 (22)	0.35 (42)	0.22 (42)	0.26 (42)
-26	-0.04 (57)	-0.08 (58)	-0.15 (58)	-0.05 (23)	-0.21 (23)	-0.38 (22)	0.31 (42)	0.20 (42)	0.23 (42)
-27	-0.05 (57)	-0.09 (58)	-0.16 (58)	-0.02 (23)	-0.20 (23)	-0.38 (22)	0.55 (41)	0.26 (41)	0.47 (41)
-28	0.05 (56)	-0.10 (57)	-0.03 (57)	0.01 (23)	-0.18 (23)	-0.34 (22)	0.50 (41)	0.23 (41)	0.46 (41)
-29	0.03 (56)	-0.09 (57)	-0.02 (57)	0.01 (23)	-0.19 (23)	-0.32 (22)	0.45 (41)	0.18 (41)	0.45 (41)
-30	0.05 (55)	-0.01 (56)	-0.07 (56)	0.04 (23)	-0.16 (23)	-0.26 (22)	0.58 (39)	0.08 (39)	0.55 (39)
-31	0.14 (53)	-0.17 (54)	-0.07 (54)	-0.01 (22)	-0.21 (22)	-0.31 (21)	0.38 (36)	-0.06 (36)	0.39 (36)

Table S3. Pearson correlation between the INP concentration and CFA/IC parameters of the complete data set. Bold coefficients indicate a significant correlation ($p < 0.05$). The number of samples is given in parenthesis.

		-20 °C	-23 °C	-24 °C	-25 °C	-26 °C	-27 °C	-28 °C	-30 °C
CFA	dust	-0.11 (57)	0.19 (121)	0.26 (125)	0.27 (125)	0.21 (125)	0.24 (124)	0.31 (123)	0.34 (120)
CFA	conductivity	-0.04 (58)	0.15 (122)	0.20 (126)	0.20 (126)	0.15 (126)	0.11 (125)	0.14 (124)	0.04 (121)
CFA	Ca ²⁺	-0.16 (58)	0.06 (121)	0.12 (125)	0.12 (125)	0.07 (125)	0.09 (124)	0.18 (123)	0.20 (120)
CFA	Na ⁺	0.01 (48)	0.01 (105)	0.04 (107)	0.03 (107)	0.00 (107)	-0.04 (106)	-0.03 (105)	-0.08 (103)
CFA	NH ₄ ⁺	-0.09 (55)	-0.02 (112)	0.01 (116)	0.02 (116)	0.01 (116)	0.06 (115)	0.11 (114)	0.05 (111)
CFA	NO ₃ ⁻	-0.11 (55)	0.00 (113)	0.01 (116)	0.00 (116)	-0.01 (116)	0.04 (115)	0.12 (114)	0.18 (111)
IC	Ca ²⁺	-0.10 (61)	0.05 (126)	0.10 (130)	0.11 (130)	0.09 (130)	0.09 (129)	0.17 (128)	0.13 (125)
IC	Na ⁺	-0.01 (61)	-0.01 (126)	-0.01 (130)	0.00 (130)	0.00 (130)	0.00 (129)	0.03 (128)	0.03 (125)
IC	NH ₄ ⁺	-0.10 (61)	-0.02 (126)	0.02 (130)	0.02 (130)	0.01 (130)	0.06 (129)	0.15 (128)	0.06 (125)
IC	NO ₃ ⁻	-0.01 (61)	-0.06 (126)	-0.05 (130)	-0.06 (130)	-0.07 (130)	-0.05 (129)	0.01 (128)	0.01 (125)
IC	K ⁺	-0.04 (61)	0.00 (126)	0.01 (130)	0.01 (130)	0.00 (130)	0.02 (129)	0.04 (128)	0.03 (125)
IC	Mg ²⁺	-0.05 (61)	0.01 (126)	0.01 (130)	0.01 (130)	0.01 (130)	-0.03 (129)	0.03 (128)	-0.02 (125)
IC	F ⁻	-0.04 (34)	0.00 (69)	0.00 (70)	0.02 (70)	0.08 (70)	0.11 (70)	0.24 (69)	0.29 (66)
IC	MSA ⁻	-0.15 (34)	-0.10 (61)	-0.10 (63)	-0.11 (63)	-0.09 (623)	0.04 (62)	0.08 (62)	0.11 (62)
IC	Cl ⁻	-0.07 (61)	-0.01 (126)	0.00 (130)	0.01 (130)	0.00 (130)	-0.01 (129)	0.02 (128)	0.01 (125)
IC	Br ⁻	-0.07 (46)	0.12 (96)	0.10 (99)	0.08 (99)	0.06 (99)	-0.12 (98)	-0.07 (97)	-0.01 (96)
IC	SO ₄ ²⁻	-0.07 (61)	-0.01 (126)	0.03 (130)	0.03 (130)	0.02 (130)	0.01 (129)	0.07 (128)	-0.03 (125)

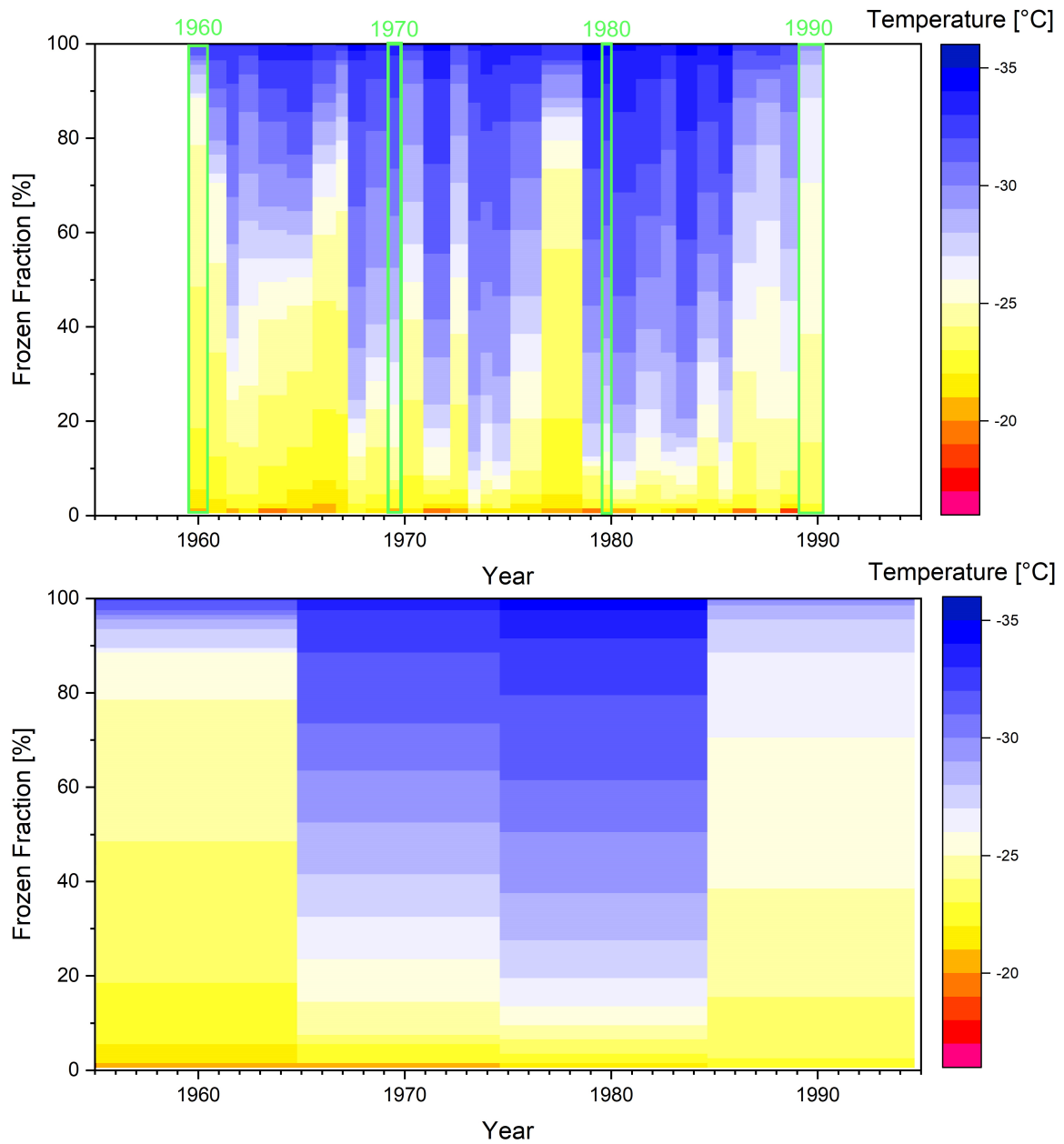


Figure S1. Qualitative comparison of the freezing spectra with regards of the two general sampling frequencies (top: 1 sample per year, bottom: 1 sample every ten years). The four samples of the lower sampling frequency (bottom layer and highlighted in green on the top layer) qualitatively reflect the higher frequency data well.

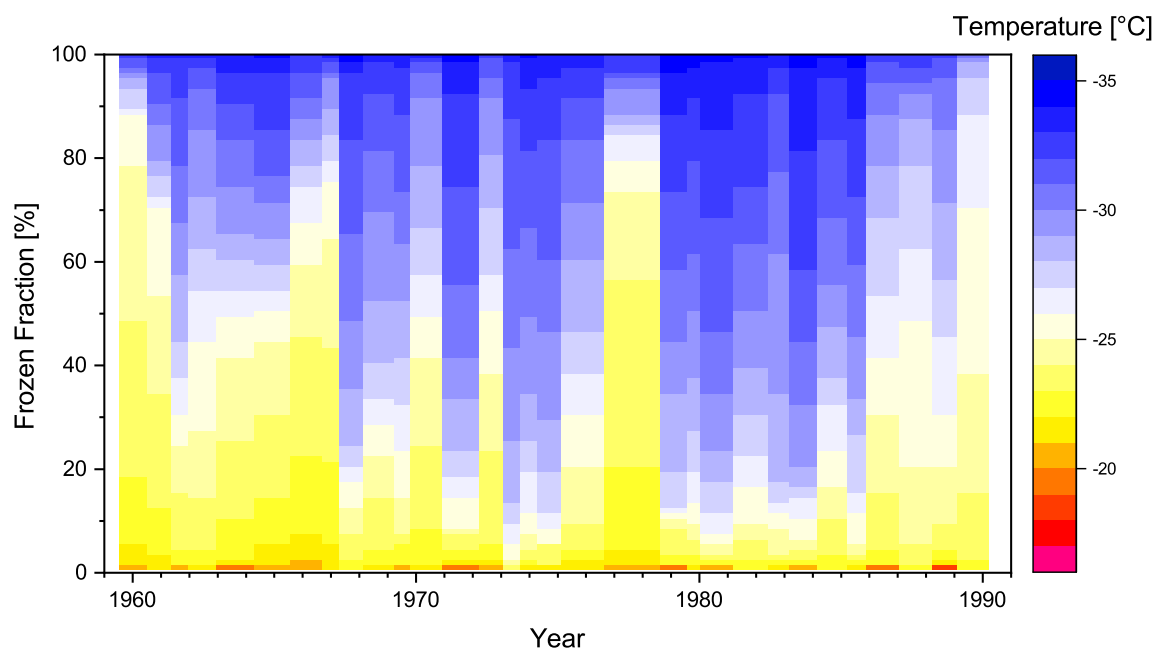


Figure S2. Frozen fractions of the modern day samples depending on freezing temperature (colors). The data points are not interpolated in time.

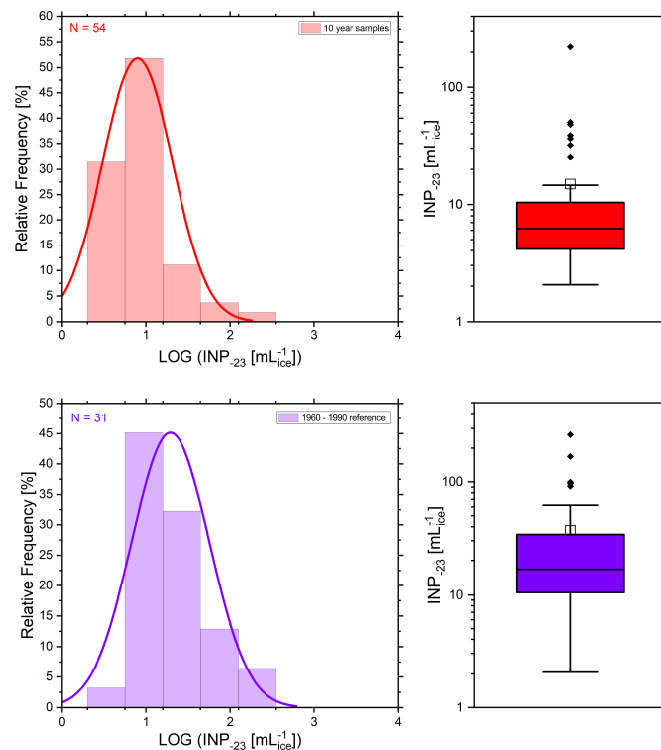


Figure S3. Empiric probability density function (bars) of the logarithmic INP concentration at $-23\text{ }^{\circ}\text{C}$ of the 10 year samples (top, red) and the modern day samples (bottom, purple). The data follows a log-normal distribution (fitted curve). The right panel shows the corresponding Box-Whisker plot.

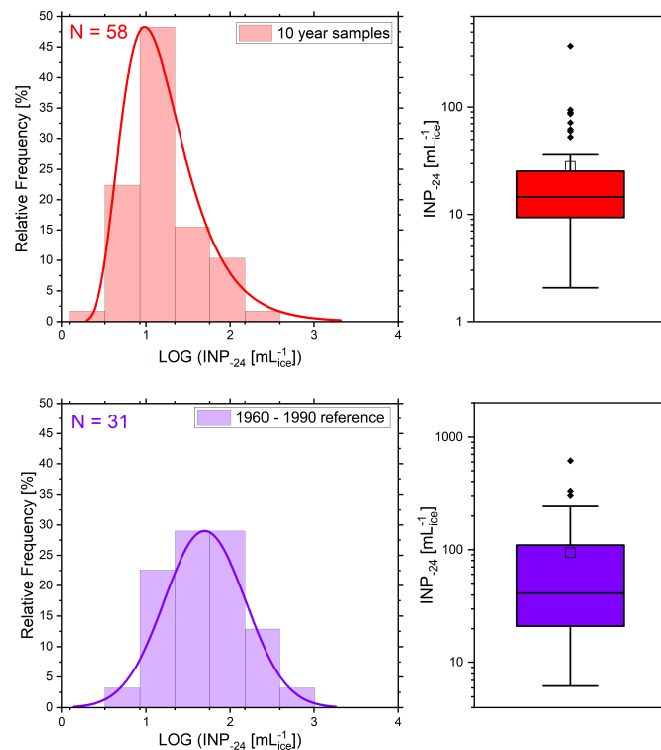


Figure S4. Empiric probability density function (bars) of the logarithmic INP concentration at $-24\text{ }^{\circ}\text{C}$ of the 10 year samples (top, red) and the modern day samples (bottom, purple). The data follows a log-normal distribution (fitted curve). The right panel shows the corresponding Box-Whisker plot.

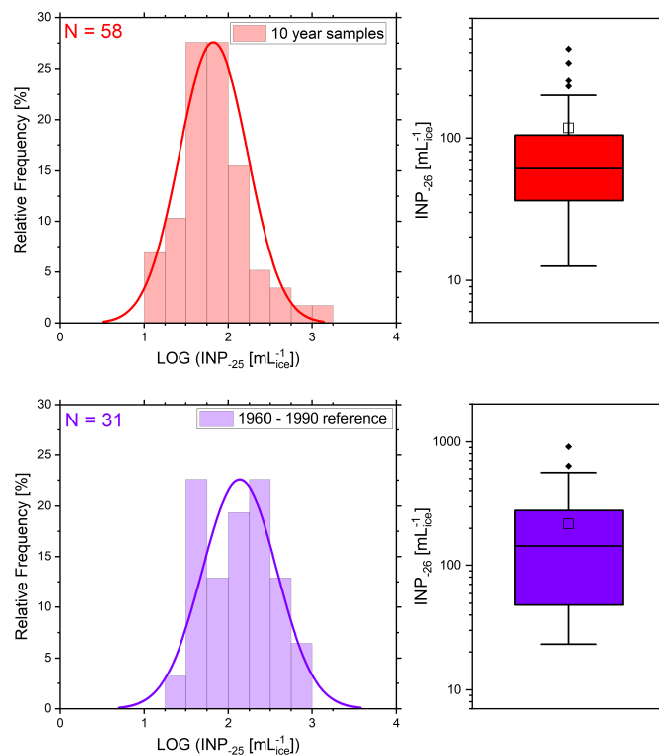


Figure S5. Empiric probability density function (bars) of the logarithmic INP concentration at $-26\text{ }^{\circ}\text{C}$ of the 10 year samples (top, red) and the modern day samples (bottom, purple). The data follows a log-normal distribution (fitted curve). The right panel shows the corresponding Box-Whisker plot.

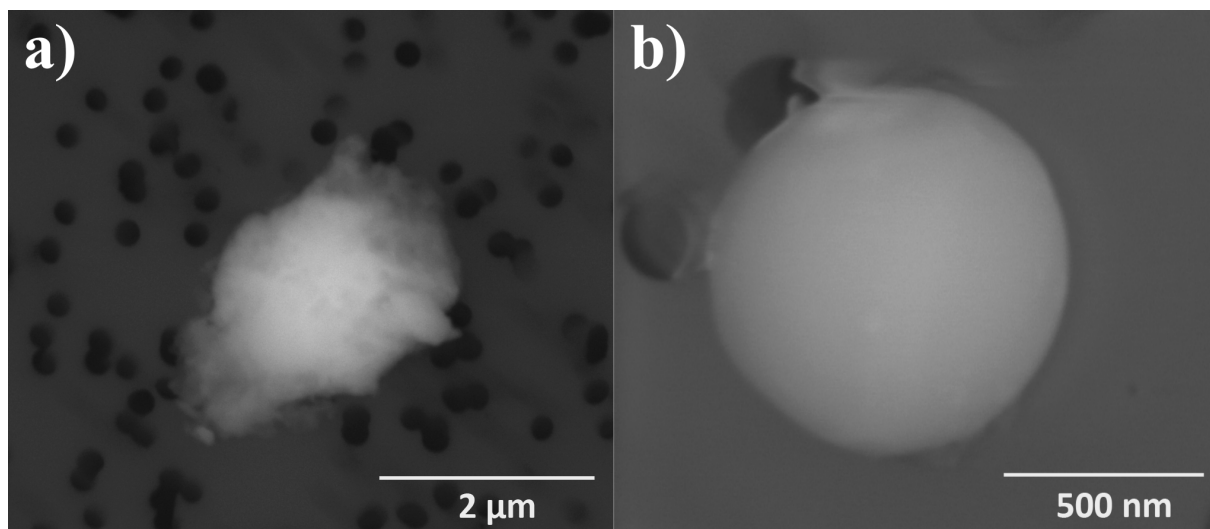


Figure S6. Scanning electron microscope image of an aluminosilicate particle (a) and a fly ash particle (b) from the 1977 sample.